Mono- and Bis-Type NS₂-Donor Macrocyclic Fluoroionophores Exhibiting Mercury(II)-Selectivity

Sunhong Park, Chul Soon Park, Seul-Gi Lee, and Shim Sung Lee[*]

Department of Chemistry and Research Institute of Natural Science, Gyeongsang National University, Jinju 660-701, Korea
*[*]E-mail: sslee@gnu.ac.kr*

Mercury(II) is considered as one of the most toxic heavy metal species for the human health and environment because it can be widely distributed in air, water, soil, food, and industrial products.[1] Thus, the design and syntheses of chemosensors for mercury(II) detection has received considerable attention.[2] Owing to their selective complexation with metal ions as well as great structural variety, macrocycic ligands make them ideal candidates in the receptor part of the chemosensors including chromo- and fluoroionophores.[3] In this reagrds, many efforts have been devoted to the syntheses of new macrocyclic receptors for Hg²⁺.[4]

On the other hand, a range of heavy metal complexes of sulfur-containing mixed-donor macrocycles featuring supramolecular structures have been reported by us[5] and other groups.[6] For example, we recently reported a series of isomeric NS₂-donor macrocycles including a *meta*-type isomer **L¹** which show a unique leaf-shaped infinite 1D structure on complexation with mercury(II) halides.[7a] In this case, one mercury(II) center has a distorted trigonal bipyramidal environment with coordination sites occupied by the facial mode of NS₂-donors from one **L¹** and the two remaining sites are occupied by two halide ions. More recently, we also synthesized Hg²⁺ complexes of **L¹** which also gave rise to different coordination modes and topologies.[7b] Sandwich-type Hg²⁺ complexes of **L¹**, [Hg(**L¹**)₂]X₂ (X = NO₃ or ClO₄), and Ag(I)/Pd(II) heteronuclear 2D network complex was also obtained in which [*cis*-Cl₂Pd(**L¹**)] acts as a metallo-ligand.[7b]
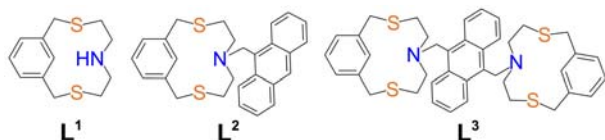
Based on the above, we have been interested in extending these results in the macrocycle-based approach to develop fluoroionophores for Hg²⁺. Most systems using fluorescence spectroscopy for detecting Hg²⁺ are based on the complexation enhancement of the fluorescence quenching effect (CHEQ; *on-off* or *turn-off* type).[7] In spite of the important implications for the practical use, however, a few fluoroionophores are based on the fluorescence enhancement upon chelation effect (CHEF; *off-on* or *turn-on*

type). In connection with this reason, we modified **L¹** with *N*-anthracenylmethyl group to give **L²** and further carried out the synthesis of new bis-type macrocyclic[8] analog **L³** as *turn-on* type fluoroionophore.

Experimental Section

General. All commercial reagents including solvents were of analytical reagent grade where available. NMR spectra were recorded on a Bruker DRX-300 spectrometer (300 MHz). The mass data were obtained on an Applied Biosystems 4000 Q TRAP (ESI) at the Central Instrument Facility of Gyeongsang National University. Fluorescence emission spectra were recorded with a Shimadzu RF-5301-PC instrument.

Synthesis of L². 9-Bromomethylanthracene (0.34 g, 1.3 mmol), **L¹** (0.26 g, 1.1 mmol) and K₂CO₃ (0.46 g, 3.3 mmol) were dissolved in dry acetonitrile (50 mL). The reaction mixture was refluxed under stirring overnight. After the reaction was completed, the filtrate was evaporated and the residue was partitioned between water and dichloromethane. The aqueous phase was separated and extracted with two further portions of dichloromethane. The organic fractions were combined and dried over Na₂SO₄. After evaporation of the solvent, crude product was subjected to column chromatography (SiO₂; 5% ethyl acetate/*n*-hexane) and yielded pure **L²** as yellow solid (0.26 g, 55%). ¹H-NMR (300 MHz, CDCl₃): δ 7.15-8.37 (m, 13H, anthracene & aromatic), 4.47 (s, 2H, NCH_2-anthracene), 3.71 (s, 4H, ArCH_2S), 2.35-2.39 (m, 4H, NCH_2CH₂S, J = 3.4 Hz), 2.26-2.30 (m, 4H, NCH₂CH_2S, J = 3.4 Hz). ¹³C-NMR (75 MHz, CDCl₃): δ 137.9, 131.4, 132.2, 130.5, 130.3, 129.9, 129.1, 128.0, 127.7, 125.8, 124.9, 124.7, 51.8, 49.5, 36.0, 26.2 ppm. ESI-MS *m/z* (MH⁺) 430.6 (calcd 430.2).

Synthesis of L³. The synthetic procedure was almost the same as for **L²** except for the use of 9,10-bis(bromomethyl)-anthracene (0.36 g, 1.0 mmol) and **L¹** (0.50 g, 2.1 mmol). Column chromatography (SiO₂; 5% ethyl acetate/*n*-hexane) afforded the product as a yellow solid (0.34 g, 61%). ¹H-NMR (300 MHz, CDCl₃): δ 7.15-8.31 (m, 16H, anthracene & aromatic), 4.46 (s, 4H, NCH_2-anthracene), 3.71 (s, 8H, ArCH_2S), 2.34-2.39 (m, 8H, NCH_2CH₂S, J = 3.4 Hz), 2.25-2.29 (m, 8H, NCH₂CH_2S, J = 3.4 Hz). ¹³C-NMR (75 MHz,

**Table 1.** Crystal Data and Structural Refinement for **L^2**

Empirical formula	C$_{27}$H$_{27}$NS$_2$
Fw	429.62
Crystal system	Monoclinic
Space group	$P2_1/c$
a /Å	11.4189(7)
b /Å	20.350 (1)
c /Å	9.3548(6)
α /°	90
β /°	97.038 (1)
γ /°	90
V /Å^3	2157.4(2)
Z	4
D_{calc} / g cm^{-3}	1.323
$F(000)$	912
μ /mm^{-1}	0.262
θ range /°	1.80-27.00
Reflns collected (R_{int})	13165 (0.0533)
Independent reflns	4686
R_1; wR_2 [$I > 2\sigma(I)$]	0.0397, 0.0875
R_1; wR_2 (all data)	0.0776, 0.1013
GOF (F^2)	1.022

CDCl$_3$): δ 137.7, 130.9, 130.8, 130.5, 130.2, 128.0, 125.3, 125.1, 51.6, 36.0, 26.2 ppm. ESI-MS *m/z* (MH$^+$) 681.8 (calcd 681.2).

Crystallography. A crystal suitable for X-ray diffraction was mounted on a Bruker SMART diffractometer equipped with a graphite monochromated Mo Kα (λ = 0.71073 Å) radiation source and a CCD detector. The frame data were processed to give structure factors by the program SAINT.[9] The intensity data were corrected for Lorentz and polarization effects. The structures were solved by a combination of the direct method and the difference Fourier methods provided by the program package SHELXTL,[10] and refined using a full matrix least square against F^2 for all data. All the non-H atoms were refined anisotropically. All hydrogen atoms were included in calculated positions with isotropic thermal parameters 1.2 times those of attached atoms. Crystallographic data are summarized in Table 1.

Results and Discussion

Syntheses of Fluorescence Ligands. The parent macrocycle **L^1** was synthesized by a dithiol-dibromide coupling reaction of **1** and α,α'-dibromo-*m*-xylene followed by deprotection of the Boc-group as previously reported by us (Scheme 1).[11] The reaction of **L^1** with 9-(bromomethyl)-anthracene afforded the desired fluorescence macrocycle **L^2**. The dilinked macrocyclic analogue **L^3** was prepared from the parallel reaction with 9,10-bis(bromomethyl)anthracene in a reasonable yield. The target macrocycles were purified by silica-gel column chromatography in good yields. Their ^{1}H and ^{13}C NMR spectra exhibit characteristic singlets at 4.47 (**L^2**), 4.46 (**L^3**), and 51.8 (**L^2**) and 51.6 (**L^3**) ppm, respectively, arising from the each methylene protons bet-
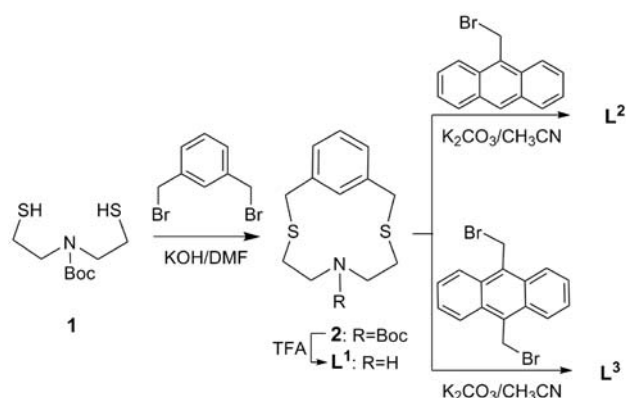
Scheme 1. Synthetic route to **L^2** and **L^3**.
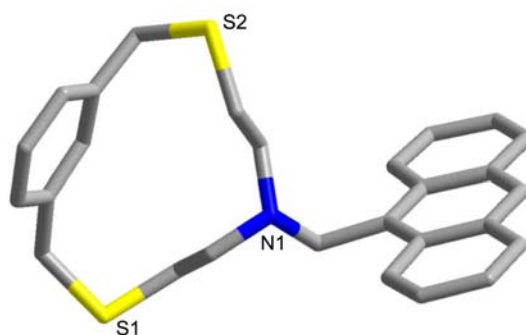
Figure 1. Crystal structure of **L^2**.

ween *tert*-N and anthracene unit (see Supporting Information).

The structure of **L^2** was also characterized in the solid state by single crystal X-ray crystallography (Figure 1). Single crystals of **L^2** suitable for X-ray analysis were obtained by slow evaporation from the solution of dichloromethane. In crystal structure, the N and two S-donors are arranged exodentate with respect to the ring cavity, with the macrocycle adopting a slightly folded arrangement over the xylyl subunit. The S1···S2 distance in a ring is 6.584(1) Å. The aliphatic ring segment corresponding to S1-C-C-N1-C-C-S2 shows an *anti-anti* arrangement between two adjacent donors in keeping with the restricted nature of this ring.

Cation-Induced Fluorescence Spectra. As a preliminary tool, the cation sensing as fluorescent sensors toward diverse metal ions (5.0 equiv) was examined for **L^2** and **L^3** (excitation at 368 nm). The fluorescent responses to the diverse metal ions as perchlorate salts under the same conditions are shown in Figure 2. Free **L^2** and **L^3** both exhibit weak fluorescence due to the photoinduced electron transfer (PET) quenching by the lone-pair of electrons on the *tert*-N atoms in each ligand. Importantly, the addition of Hg^{2+} resulted in the maximum chelation enhanced fluorescence (CHEF) effect for **L^2** (Figure 2(a)) and **L^3** (Figure 2(b)). In both cases, the typical structured band pattern in 380-500 nm arising from the anthracene unit was apparent. The group IA, IIA and *d*-block transition metal ions, however, showed either no or only a small influence on the fluorescence intensity. In other words, upon Hg^{2+} binding a strong fluorescence emission is clearly visible to the naked eye, as can be seen in
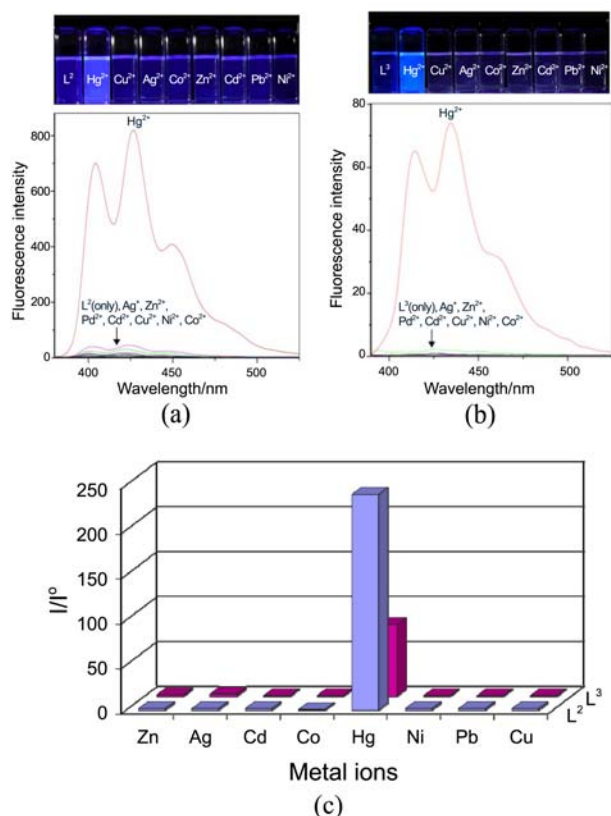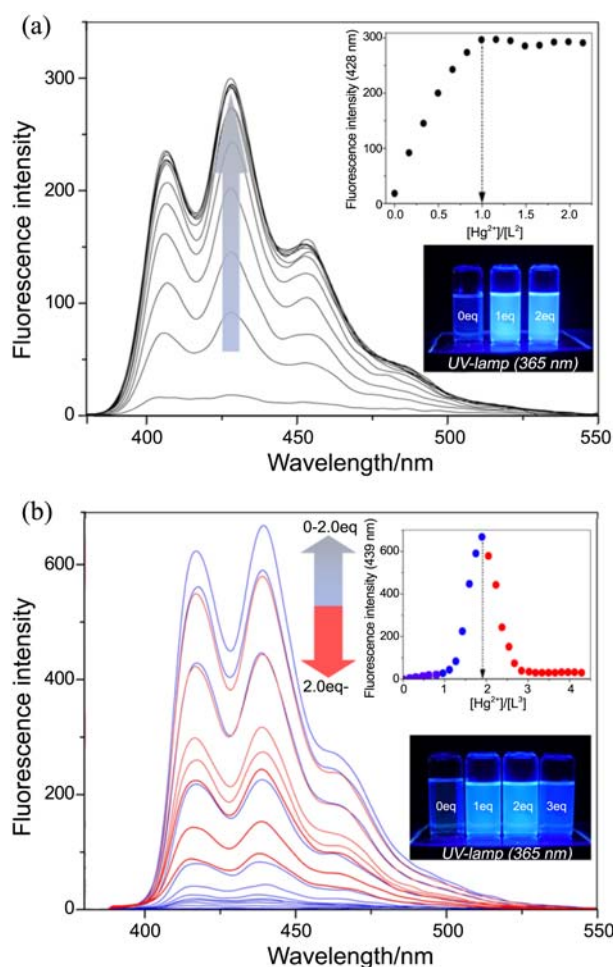
Figure 2. Fluorescence spectra of (a) $\mathbf{L^2}$ and (b) $\mathbf{L^3}$ (20 μM) in the presence of the metal perchlorates (5.0 equiv), and (c) normalized intensity ($\mathbf{I/I^o}$) in acetonitrile.

Figure 3. Fluorescence titrations of (a) $\mathbf{L^2}$ and (b) $\mathbf{L^3}$ with $Hg(ClO_4)_2 \cdot 3H_2O$ in acetonitrile. The insects show the fluorescence intensity at 428 nm for $\mathbf{L^2}$ and 439 nm for $\mathbf{L^3}$. [ligand] = 2.0×10^{-5} M, λ_{ex} = 365 nm.

the photograph (Figures 2(a) and 2(b)).

It is instructive to compare the results for $\mathbf{L^2}$ and $\mathbf{L^3}$. Overall, the CHEF effect induced by Hg^{2+} was found to fall in the order $\mathbf{L^2}$ (256) > $\mathbf{L^3}$ (81), where the values in parentheses are the normalized intensities ($\mathbf{I/I^o}$) (Figure 2(c)). Upon complexation, the changes of λ_{max} for each of the other metal ions were negligible indicating that none of these metal ions influence the HOMO and LUMO levels of each ligand.

The effect of the Hg^{2+} complex formation on the photophysical properties of the fluoroionophores was investigated by fluorescence titrations (Figure 3). The complex formation of $\mathbf{L^2}$ and $\mathbf{L^3}$ were clearly observed when each fluoroionophore was titrated with $Hg(ClO_4)_2$. In each case, the initial addition of the Hg^{2+} caused an increase in the fluorescence intensity. The titration plots (insets of Figure 3) show that these changes occur until the addition of 1.0 equiv of Hg^{2+} for $\mathbf{L^2}$ (Figure 3(a)) and 2.0 equiv for $\mathbf{L^3}$ (Figure 3(b)).

In case of $\mathbf{L^2}$, as seen in the inset of Figure 3(a), the emission intensity at 428 nm monotonically increases with the addition of Hg^{2+} while no obvious shift or change in the shape of the maximum emission is observed. Linearity between the fluorescence intensity and the concentration of Hg^{2+} from 0 to 1.0 equiv is established, and then the titration plot achieved a plateau, suggesting a 1:1 (metal-to-ligand) complexation.

On the other hand, the emission intensity of $\mathbf{L^3}$ at 439 nm shows more complicate behavior depending on the amount of added Hg^{2+} as seen in the inset of Figure 3(b). For example, the titration of $\mathbf{L^3}$ with Hg^{2+} shows gradual enhancement in fluorescence intensity between 0-1.0 equiv of Hg^{2+} and then shows rapid increase between 1.0-2.0 equiv of Hg^{2+}. After the maximum emission at 2.0 equiv of Hg^{2+}, a rapid quenching was observed till about 3 equiv and then the intensity gradually decreased almost to the baseline. In this case, the observed maximum emission at 2.0 equiv obviously suggests a 2:1 (metal-to-ligand) complexation. And the drastic changes (increase and decrease) in the fluorescence intensity before and after the 2.0 equiv of Hg^{2+} can be explained that the $[Hg_2(\mathbf{L^3})]^{4+}$ exhibits the strongest fluorescence intensity among the species formed in the titration stage such as $\mathbf{L^3}$, $[Hg(\mathbf{L^3})]^{2+}$, and $[Hg_3(\mathbf{L^3})]^{6+}$. Some of these species were also confirmed by ESI-mass data (Figure 4).

ESI-Mass Data of Hg(II) Complexes. The relationship between structure and properties is the critical issue in functional supramolecular system including the chemosensor area. However, our repeated effort to obtain the crystal structures of the corresponding complexes was not success-
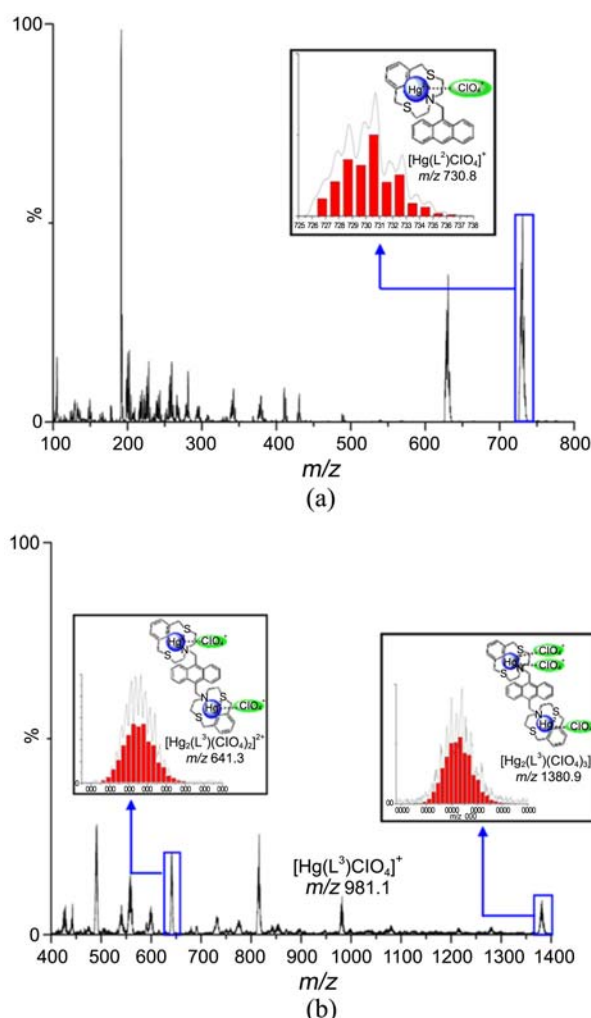
Figure 4. ESI-mass data of (a) **L²** and (b) **L³** in the presence of $Hg(ClO_4)_2$ in acetonitrile.

ful. Instead, the binding behavior of the ligands toward Hg^{2+} was further investigated by ESI-mass technique (Figure 4). The observed 1:1 stoichiometry for the complexation of **L²** with Hg^{2+} (Figure 3(a)) was also confirmed, which correspond to the species $[Hg(\mathbf{L^2})ClO_4]^+$ (*m/z* 730.8) (Figure 4(a)). The observed 2:1 stoichiometry for complexation of **L³** with Hg^{2+} is also confirmed by the corresponding complex solutions, which correspond to the species $[Hg_2(\mathbf{L^3})(ClO_4)_3]^+$ (*m/z* 1380.9) (Figure 4(b)). These peaks are also verified by comparison of the relative abundance of their isotope peak patterns between the observed peaks and the corresponding theoretical simulation. Again, it is noted that the unique behavior of the proposed ligand system can be thus be attributed to its selective complexation affinity for mercury(II).

In summary, mono- and bis-macrocyclic fluoroionophores with NS₂-donor sets were synthesized. Both of fluoroionophores show Hg^{2+} selectivity through a strong CHEF effect (or *turn-on*). The mono-ring fluoroionophore shows relatively higher selectivity than that of bis-ring analog. The mono-ring derivative exhibits '*off-on*' behavior while the bis-ring

derivative is characterized by unique '*off-on-off*' behavior due to the different photophysical properties of the species. The results of the ESI-mass experiment confirmed the existence of some stoichiometric species.

Supplementary Materials. CCDC 842824 (**L²**) contains the supplementary crystallographic data. These data can be obtained free of charge *via* www.ccdc.cam.ac.uk/ data_request/cif, by emailing data_request@ccdc.cam.ac.uk, or by contacting The Cambridge Crystallographic data Centre, 12, Union Road, Cambridge CB2 1EZ, UK; fax: +44 1223 336033.

References

1. (a) ATSDR, *Toxicological Profile for Mercury*, U. S. Department of Health and Human Services, Atlanta, GA, 1999. (b) Clarkson, T. W.; Magos, L. *Crit. Rev. Toxicol.* **2006**, *36*, 609.
2. (a) Santra, M.; Ryu, D.; Chatterjee, A.; Ko, S.-K.; Shin, I.; Ahn, K. H. *Chem. Commun.* **2009**, 2115. (b) Wang, H.; Chan, W.-H. *Tetrahedron* **2007**, *63*, 8825. (c) Chen, X.; Kim, S.-W.; Jou, M. J.; Kim, Y.; Kim, S.-J.; Park, S.; Yoon, J. *Org. Lett.* **2008**, *10*, 5235.
3. (a) Vance, D. H.; Czarnik, A. W. *J. Am. Chem. Soc.* **1993**, *115*, 12165. (b) de Silva, A. P.; Fox, D. B.; Huxley, A. J. M.; Moody, T. S. *Coord. Chem. Rev.* **2000**, *205*, 41. (c) Iwata, S.; Matsuoka, H.; Tanaka, K. *J. Chem. Soc., Perkin Trans. 1* **1997**, 1357. (d) Santis, G. D.; Fabbrizzi, L.; Licchelli, M.; Mangano, C.; Sacchi, D.; Sardone, N. *Inong. Chim. Acta* **1997**, *257*, 69.
4. (a) Sancenón, F.; Martínez-Máñez, R.; Soto, J. *Angew. Chem., Int. Ed.* **2002**, *41*, 1416. (b) Lee, J.-E.; Choi, K. S.; Seo, M. L.; Lee, S. S. *Bull. Korean Chem. Soc.* **2010**, *31*, 2031.
5. (a) Lindoy, L. F.; Meehan, G. V.; Vasilescu, I. M.; Kim, H. J.; Lee, J.-E.; Lee, S. S. *Coord. Chem. Rev.* **2010**, *254*, 1713. (b) Lee, S. J.; Jung, J. H.; Seo, J.; Yoon, I.; Park, K.-M.; Lindoy, L. F.; Lee, S. S. *Org. Lett.* **2006**, *8*, 1641.
6. (a) Wolfe, S. *Acc. Chem. Res.* **1972**, *5*, 102. (b) Wolf, R. E., Jr.; Hartman, J. R.; Storey, J. M. E.; Foxman, B. M.; Cooper, S. R. *J. Am. Chem. Soc.* **1987**, *109*, 4328. (c) Buter, J.; Kellog, R. M.; van Bolhuis, F. *J. Chem. Soc., Chem. Commun.* **1991**, 910. (d) Geue, R.; Jacobson, S. H.; Pizer, R. *J. Am. Chem. Soc.* **1986**, *108*, 1150.
7. (a) Park, S.; Lee, S. Y.; Jo, M.; Lee, J. Y.; Lee, S. S. *CrystEngComm* **2009**, *11*, 43. (b) Park, S.; Lee, S. Y.; Lee, S. S. *Inorg. Chem.* **2010**, *49*, 1238.
8. (a) Jin, Y.; Yoon, I.; Seo, J.; Lee, J.-E.; Moon, S.-T.; Kim, J.; Han, S. W.; Park, K.-M.; Lindoy, L. F.; Lee, S. S. *Dalton Trans.* **2005**, 788. (b) Kim, H. J.; Jin, Y.; Seo, J.; Lee, J.-E.; Lee, J. Y.; Lee, S. S. *Inorg. Chem. Commun.* **2006**, *9*, 1040. (c) Lee, J.-E.; Jin, Y.; Seo, J.; Yoon, I.; Song, M. R.; Lee, S. Y.; Park, K.-M.; Lee, S. S. *Bull. Korean Chem. Soc.* **2006**, *27*, 203. (d) Lee, J.-E.; Lee, E. Kang, Y. J.; Park, K.-M.; Lee, S. S. *Bull. Korean Chem. Soc.* **2011**, *32*, 1761.
9. Bruker, SMART and SAINT: *Area Detector Control and Integration Software Ver. 5.0*; Bruker Analytical X-ray Instruments: Madison, Wisconsin, 1998.
10. Bruker, SHELXTL: *Structure Determination Programs Ver. 5.16*; Bruker Analytical X-ray Instruments: Madison, Wisconsin, 1998.
11. Chartres, J. D.; Groth, A. M.; Lindoy, L. F.; Lowe, M. P.; Meehan, G. V. *J. Chem. Soc., Perkin Trans.* **2000**, *1*, 3444.